HIGH RESOLUTION OBSERVATIONS OF SOLAR FLARES

B. Sylwester[1]

[1]*Space Research Centre, Polish Academy of Sciences, Kopernika 11, 51-622 Wroclaw,Poland*

ABSTRACT

Over the past few years, our team in Space Research Center (SRC) of Polish Academy of Sciences in Wroclaw has been interested in developing numerical image enhancement techniques with the aim of increasing the resolution on SXT flare images. The algorithm (ANDRIL) has been developed which allows for the image deblurring with over sampling. The application of this algorithm allows an increase in the resolution of the SXT images to the level of ~ 1 arcsec. We performed the deconvolution of a large number of flare sequences using ANDRIL algorithm. The analysis of these data allowed to study the morphology of million degree flaring plasma with the resolution comparable to *TRACE.* In order to infer the thermodynamic parameters of the plasma from the analysis of deconvolved images their precise co-alignment is required. Techniques which have been developed at SRC to achieve high accuracy of image co-alignment will be discussed. The application of the filter ratio technique to the deconvolved and co-aligned images allows the study of the temperature and emission measure distributions of the flaring plasma in great detail. These maps better resolve flare kernels located both at the summits and footpoints of flaring loop structures. The main results obtained will be presented in the review.

OVERVIEW

From the early days of X-ray corona observations it was clear that there is an association between the location of the structures observed in the corona and the pattern of features seen on the solar disc. It has been understood that this connection relates with the magnetic activity. The most energetic phenomena associated with the magnetic activity are solar flares usually observed within active regions. Even 30 years ago the spatial resolving power of ground based observations routinely achieved arcsec resolution. At that time the techniques of X-ray observations were only beginning to be developed and the resolution of the corona was only a few arcmins at best.

The era of satellite borne experiments with the X-ray detectors on-board begun in 1962 when the first (from a series of eight) *Orbiting Solar Observatories* (*OSO 1*) has been launched. Among the significant achievements of this program were the first full-disc photographs of the solar X-ray corona and the first X-ray observations of a solar flare. The launch of the first manned observatory *Skylab* in 1973, marked a beginning of the new era in the investigation of solar short wavelength radiation. The *Skylab* X-ray and EUV images provided convincing evidence and confirmation of results from sounding rockets (obtained in the late 1960s and early 1970s), that the corona is comprised mostly of magnetic loops and arches (Sheely et al., 1975, Foukal, 1976). From that time the coronal loops are often referred to as the fundamental building blocks of the magnetically dominated quiet and active corona. The disadvantages of the *Skylab* mission is that it took place during a period of low flare activity and the image recording medium used was photographic plates. In February 1980 the NASA *Solar Maximum Mission* (*SMM*) was launched carrying eight instruments developed by international teams. The HXIS and FCS instruments on board the *SMM* allowed for imaging the flares in hard and soft X-ray ranges. The BCS provided high-resolution spectra around Fe XXV-XXVI and Ca XIX resonance lines. The HXBS allowed for observing the hard X-ray spectra of solar flares. The HXIS, FCS and BCS spectrometers on *SMM* were among the highest resolution instruments making systematic solar X-ray observations at that time. The Japanese rotationally modulated telescope on board the *Hinotori* spacecraft launched in 1981 and devoted for imaging solar flares in hard X-rays (5 - 40 keV) had similar resolution. The launch of *Yohkoh* constituted another milestone in the studies of high-temperature flare plasma. Important support to *Yohkoh* came from the EIT, CDS and SUMMER on *SOHO* and more recently from *TRACE*. In the meantime a number of sounding rocket flights carrying high resolution experiments have been launched. Although allowing for a few minutes of observing time only they made it possible to test new observing techniques in the X-ray and EUV ranges and provided the images with the best ever spatial resolution. Among these sounding rocket experiments we should mention the innovative HRTS (High Resolution Telescope and Spectrograph) instrument, NIXT X-ray imager (Normal Incidence X-ray Telescope), MSSTA (Multi-Spectral Solar Telescope Array), SERTS (Solar Extreme-ultraviolet Rocket Telescope and Spectrograph). In particular the disc X-ray flare recorded by NIXT on 11 Sept. 1989 with 0.75 arcsec resolution has been extensively studied in many papers (Golub et al., 1990, Herant et al., 1991, Golub, 1992, 1997 and Sams et al., 1992).

On the Eastern hemisphere the experimental investigations of solar X-ray radiation have been undertaken by teams working in Russia (FIAN Lebedev Physical Institute in Moscow), Czech Republic (Astronomical Institute in Ondrejov) and Poland (Space Research Center in Wroclaw).

From the beginning of *Yohkoh* era Wroclaw team took part in the analysis of data from BCS, SXT and HXT instruments. During ten years of *Yohkoh* observations we have processed and analysed a wealth of data on flares using special techniques of image reconstruction and handling, worked out in Wroclaw. In this review we will emphasis the major results obtained by our group working with the *Yohkoh* solar flare data.

METHODS OF SXT IMAGE PROCESSING AND ANALYSIS

From the earlier analysis of the best high resolution flare X-ray images (Herant et al., 1991) and results of theoretical considerations (Gomez et. al., 1993) it follows that the structuring and most of physical processes operating in solar flares act on small sub-arcsecond scales, i.e. below the nominal resolution of SXT images on *Yohkoh*. As the SXT pixel dimension and FWHM of point spread function (PSF) for the grazing incidence mirror are of similar sizes it is then possible to increase the effective resolution on the images by using image reconstruction techniques. A number of methods have been worked out and presented in the literature which allow the instrumental blurring to be removed. However, there was no well documented method (except the work of Roumeliotis, 1995) which allows deblurring and over sampling to be performed simultaneously. Over sampling means that the recovered (deconvolved) picture contains more resolution elements than the original one. In the case of the SXT images we have found that a fortunate compromise between FWHM and the pixel size allows for subdivision of each SXT pixel into 5×5 subpixels. Such an over-sampling scheme results in the formal numerical increase of the nominal resolution of the SXT image down to ~ 1 arcsec (the over-sampled size of subpixel is ~ 0.5 arcsec). We developed an algorithm called ANDRIL (**A**ccelerated **N**oise **D**amped **Ri**chardson-**L**ucy) for SXT image processing. In constructing the algorithm we followed the ideas used for reconstruction of the images from the non-refurbished Hubble Space Telescope. The details of ANDRIL can be found in the papers by Sylwester et al. (1996a) and Sylwester & Sylwester (1998a, 1999a) where extensive tests of the algorithm for various synthetic input models and various shapes of PSF have been performed. An example of the application the ANDRIL algorithm to real SXT data is shown in Figure 1 where the comparison of original and deconvolved images is presented for

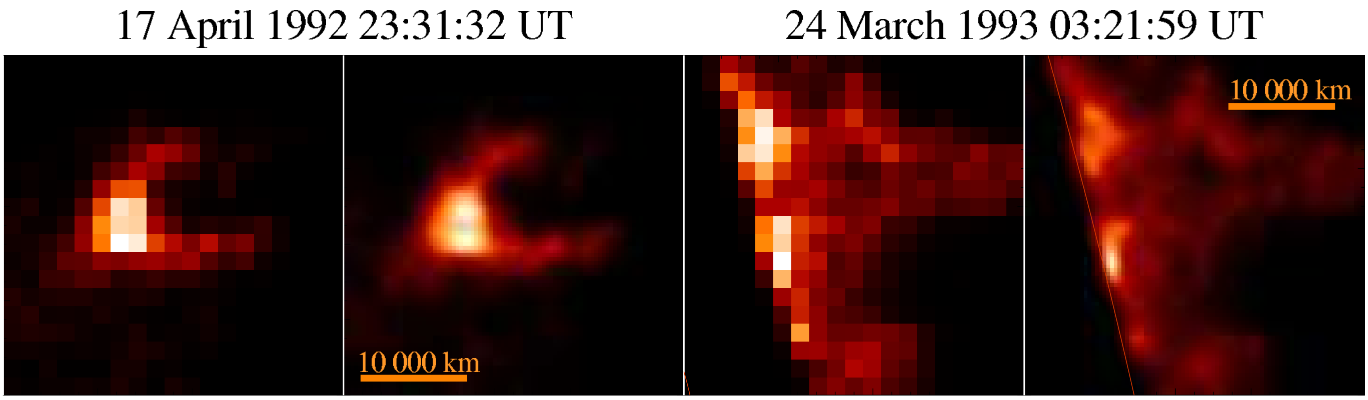

Fig. 1. *The comparison of original and deconvolved Al12 images for two flares. The original and deconvolved images have been compressed in the same way in order to reveal weaker sources. The sizes of the original images are 18×18 SXT pixels which correspond to 90×90 subpixels after the deconvolution.*

two flares (17 April 1992 during the decay phase and 24 March 1993 during the rise phase). An advantage of using ANDRIL image processing is obvious. Many fine structures of sub-arcsecond sizes can be revealed on the deconvolved images. Their physical reliability can be established when comparing the evolution on sequences of consecutive deconvolved images taken with different filters. For near the limb, the relatively simple M1.1 flare on 17 April 1992 the loop top kernel reveals double structure during the decay phase. The structure of limb C6.6 flare observed on 24 March 1993 looks more complicated. Deconvolution reveals the cusp-like structure with the main emission concentrated in one (south) foot during the rise phase.

Common interpretation of flare intensities as measured in a pair of images taken in slightly different energy bands provides information on the average temperature distribution of emitting plasma when the images are taken at the same time and the same plasma regions contribute to both bands. It is known that when image ratios are interpreted for regions of strong intensity gradients, derived values of temperatures are very sensitive to the exact co-alignment of the images in a pair. In order to better understand a dependence of derived temperature distribution on possible small misalignments of Be119 and Al12 images due to fixed accuracy of spacecraft attitude information, Sylwester (1995) investigated to what extend derived T-maps depend on the possible inaccuracy of co-alignment. Siarkowski et al. (1996) have shown that the alignment procedures used in the standard SXT image co-alignment and processing routines may be inadequate when the temperature maps are in question. In order to improve the determination of temperature pattern in the investigated structures, three numerical methods of **a**dditional **p**ointing **c**orrections (APC) settlement have been proposed and investigated.

The uncertainty of temperature determination is much larger when deconvolved SXT images are to be used as the angular resolution is increased five-fold. In the paper by Sylwester & Sylwester (2001a) a method of co-alignment of deconvolved images has been proposed for flares partially occulted by the solar disc. For these flares the limb of the solar atmosphere occults the X-ray source at the very same location for images taken using individual filters. The description of modelling of X-ray occultation process can be found in Sylwester & Sylwester (2002). Taking these results into account it is possible to co-align the images to better than 0.1 arcsec accuracy which allows for temperature determinations on subpixel scales. We will refer to this method of co-alignment as the **l**imb **p**osition **a**djustment (LPA) as it is based on the limb as a reference. We have checked that the agreement between Al12 and Be119 images improves by using the LPA method so we have decided to adopt it routinely wherever possible.

MAIN RESULTS

After tested the ANDRIL algorithm we realised that it provides a powerful tool for processing the SXT images and we began a massive analysis of flare observations. Detailed inspection of the sequences of deconvolved images revealed usually a number of fine structure details. In the most cases the flare (as seen in all SXT bands) consists of kernels which constitute well localised, small emitting sources. The radii of

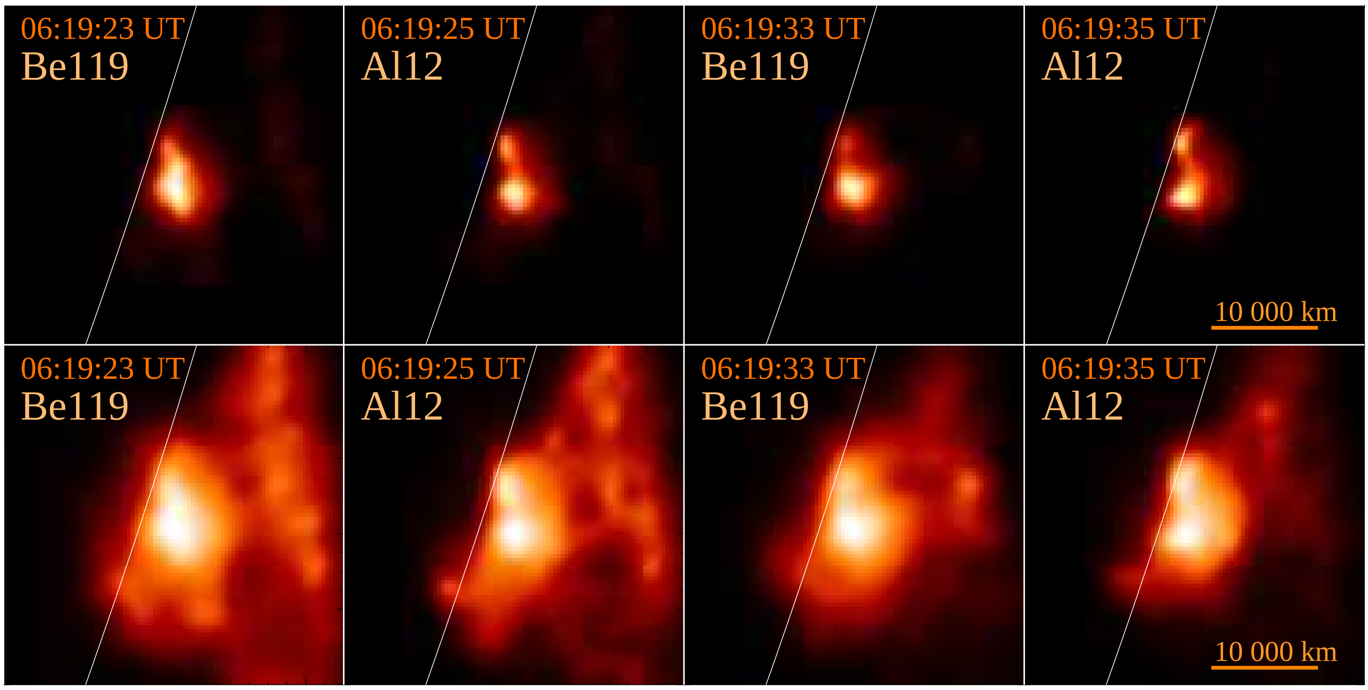

Fig. 2. *The two pairs of consecutive deconvolved and compressed Be119 and Al12 images for the 5 November 1992 limb flare. The compression scheme for the lower row images allows to see the weaker structures. The size of each image is 90×90 subpixels.*

these fine X-ray structures are of the order of $\sim$ 1 - 1.5 arcsec. Kernels are located at the summits as well as at the footpoints of flaring loops. They were identified on the original SXT images as well (Acton et al., 1992, Feldman et al., 1994a, b, Khan et al., 1995, Harra-Murnion et al., 1997, Jakimiec et al., 1998, Nitta et al., 2001). However, the deconvolved images revealed often their fine structure, which was hardly seen on the original ones (Figure 1). The top bright regions appear shortly after the flare onset and persist well into the decay phase of the flaring compact and long duration events. The soft X-ray footpoint regions (kernels) are not as well observed as the summit ones. Footpoint kernels dominate only during a short time at the flare onset and, except a few cases (Masuda et al., 1994, McTiernan et al., 1993, Hudson et al., 1994, Sylwester & Sylwester, 1998c) are not well covered by observations because of the flare trigger logging scheme used by SXT.

The deconvolved images reveal that the morphology of hot flaring plasma is usually more complicated that the theoretical flare models showing a simple loop or loop arcade connecting footpoints in the photosphere present. The flares presented in Figure 1 constitute good example. The Al12 images for the flare on 17 April 1992 during the decay and for the flare on 24 March 1993 during the rise phase reveal more complicated and nonuniform structures than those presented on theoretical sketches. The top region of the 17 April 1992 flare reveals a double structure of the kernel. The diameter of each component is $\sim$ 1300 km and their centers are separated by $\sim$ 2500 km. We have observed also flares composed of multiple coronal kernels (Sylwester et al., 1996b). The limb flare presented in the right panel of Figure 1 is relatively more complicated. The cusp-like structure, the dominating footpoint kernel and many related small emission patches located in the corona are present. This flare has been analysed by Sylwester & Sylwester (2001b). Such images convincingly suggest that simple loop structure with the emission enhanced at the top and extending towards the double footpoints at the chromosphere is not the typical pattern observed for flares. An interesting flare on 5 November 1992 (M2.0) has been analysed by Sylwester & Sylwester (1999b). The two pairs of consecutive (Be119 and Al12) deconvolved images for this event are presented in Figure 2. In the top row only the dominant kernels are seen. The lower row shows the same images but compressed in the way which allows to see much weaker structures. It is seen that the main flaring region forms a small, low-lying nonuniform emitting structure with individual knots clearly distinguished. Besides this dominant region, the enhanced emission located above (higher in the corona) and forming the ridge can be seen. Individual structures composing the ridge are seen to be connected to the main loop top kernels throughout

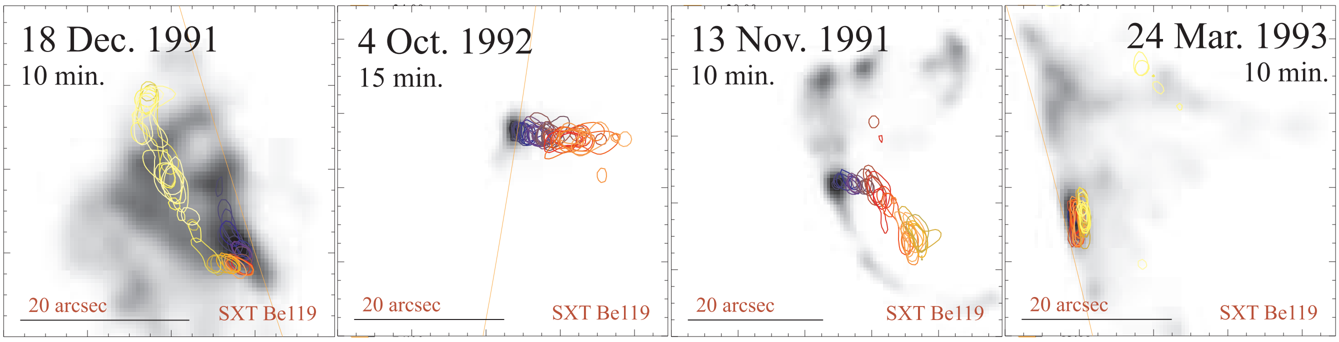

Fig. 3. *The evolution of maximum brightness location presented as shaded contours drawn at 0.9 of maximum Be119 intensity for four flares. The contours are overlaid atop the emission pattern (in grey) of the first unsaturated Be119 image within the sequence. The duration of presented evolution pattern is indicated.*

the weaker emission fringes. The ridge structure can be identified on all images obtained throughout the event's evolution. However, it is best pronounced at the beginning of flare cadence. A large number of observations similar to these presented gave birth to the rather controversial idea that a possible loop hierarchical structure of magnetic coronal fields exists (Sylwester & Sylwester, 1998b). According to this concept the magnetic field supporting the observed structures is organised into the hierarchical cascade where the larger structures are rooted at the summits (kernels) related to the smaller, lower lying structures. It is easy to interpret most of the high resolution observations of solar atmosphere within such a concept.

The inspection of sequences of SXT deconvolved images of many flares revealed that soft X-ray flare emission patterns are not only spatially complicated but also fast evolving. This is especially apparent during the flare impulsive phase. The brightest fine structures observed at the summits and at footpoints change their position during flare evolution and the solar corona appears much more dynamic than was thought before. The time variations of soft X-ray emissivity pattern based on deconvolved SXT images have been investigated by Sylwester & Sylwester (1999c, d, 2001a). We have found it convenient to follow the changes of flare brightness pattern by looking to the position of selected brightness iso-contours. The inspection of history of iso-contour locations reveals "motions" of top and footpoint kernels during the flare. In Figure 3 the changes of maximum brightness location are presented for four events. Three of them occurred at the limb which makes easy to distinguish between top and footpoint kernels while the flare on 13 November 1991 is the disc one. It is seen that during 10 - 15 min of evolution presented in the Figure the maximum emission changed its location suggesting a real motion of the kernels. For 18 December 1991 event, the observed pattern history of 10 min. evolution indicates for rather complicated arrangement of maximum brightness displacement. To clearly see the dynamics for this particular flare the reader is referred to the colour animation at `www.cbk.pan.wroc.pl/publications/2002/high_res/18dec91prod.avi`. For the flare on 4 October 1992 the movement of maximum brightness location is observed in the direction away from the Sun. The quantitative measurement of the displacement observed using Be119 filter gives a distance of about 6000 km with the corresponding velocity of not less than about 6.6 km/sec. For the disc flare on 13 November 1991 relatively large displacement of the most intense patch in the SW direction is pronounced. On the other hand for the brightest kernel of the flare on 24 March 1993 only a small apparent displacement of maximum brightness is observed. In this case the radial motions are probably substantial. A similar pattern of evolution is observed for both Al12 and Al01 images. At this point we should notice that this is not only the soft X-ray plasma that does change the location of its maximum emission during the flare evolution. When we analyse the MEM reconstructed HXT images and trace the maximum brightness location for different HXT energy channels a similar pattern of displacement as in the case of SXT images is observed. This has been illustrated for the flare on 5 October 1992 in the paper by Sylwester & Sylwester (2001a). Feldman et al. (1994b) noticed that for non impulsive flares the brightest region does not seem to move from its location at the top by more than one pixel. However, from our analysis of deconvolved images both footpoint and summit kernels as a rule displace as the event progress. Occasionally we observe the maximum brightness location to be stable for relatively long time with a following rapid change of this location (as seen through all available SXT filters). We believe these displacements are related to the real motions of plasma blobs.

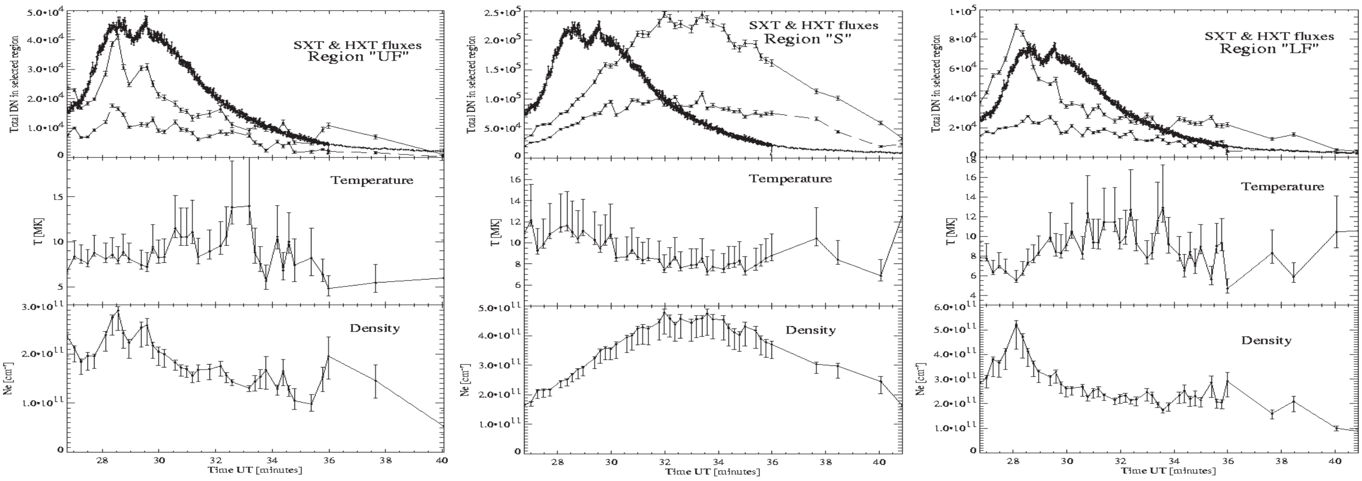

Fig. 4. *Time variations of some important characteristics for individual structures of the Masuda flare on 13 January 1992. UF (left column), S (central column) and LF (right column) denote the North footpoint (upper), summit and South footpoint (lower) kernels respectively. In the upper row the following lightcurves are displayed: HXT L channel flux multiplied by the appropriate factor in order to bring it to scale (thick line), Al12 (middle) and Be119 (bottom) SXT fluxes. The middle row shows the course of kernels' plasma temperature and the bottom row the corresponding variations of plasma density.*

The physical conditions of plasma confined in the flare kernels have been investigated by many authors. The analysis of SXT images (Acton et al., 1992, McTiernan et al., 1993, Feldman et al., 1994a, b, Doschek, Strong & Tsuneta, 1995, Tomczak, 1997, Jakimiec et al., 1998) and of spectroscopic observations (Fludra et al., 1994, Khan et al., 1995, Doschek, 1999) have been carried out. However, only the investigation of deconvolved images allows to study the plasma parameters on small scales. We have studied (Sylwester & Sylwester, 1998c, 1999b) the physical conditions within fine flaring structures observed at and near the limb. Several bright areas representing footpoint and summit kernels have been investigated. We concentrated on these images on which the dominant kernel has reached its maximum intensity. In order to determine the kernel volume we assumed a "quasi-symmetric" geometry. The integration of Al12 and Be119 fluxes for all subpixels located within the selected kernel and using filter ratio technique allowed to determine average electron temperature, emission measure and density (assuming unit filling factor). Next we investigated the physical characteristics of plasma at this location and followed their time variations.

We have analysed several limb, partly occulted flares in order to search for similarities and/or discrepancies between the temperature and emission measure patterns for the plasma confined in the foot-point and the summit volumes of flaring loops. It turned out that the kernels located at the summits are on average hotter by 2 - 3 MK in comparison with those located at the footpoint regions. Their average temperature is usually 10 - 15 MK during the rise phase and falls below 10 MK during the maximum and decay phase of the event. Their emission measures are commonly larger than those estimated for the footpoint kernels but the difference in the density is not large. However the characteristic sizes of summit kernels are larger than for footpoint ones being typically 1.5 - 2.5 arcsec diameter. The summit kernels are generally observed during the entire event evolution. The footpoint kernels as seen in soft X-rays are observed mostly during the rise and maximum phase and they usually fade-away during the decay phase. They constitute well localised, small sources with the characteristic size usually less than 1.5 arcsec. The smallest diameter of footpoint kernel as obtained from FWHM of cross sectional brightness profile was ~ 0.8 arcsec. During the rise phase the footpoint kernels are composed of dense (maximum density $\sim 1 - 5 \times 10^{11}$ cm $^{-3}$) but not especially hot (6 - 9 MK) plasma. Usually the temperature of footpoint kernels is more or less constant during the phase of intense soft X-ray emission, in the contrary to what is observed for summit kernels for which temperature tends to increase from the very beginning of the event. Later on (during the maximum and decay phase) the footpoint kernel temperature increases being comparable with the top kernels one. The time variations of characteristic parameters (soft and hard X-ray fluxes, temperature and density) for two footpoints and summit kernels are presented in Figure 4 for "canonical" Masuda flare on 13 January 1992. It is worth noting

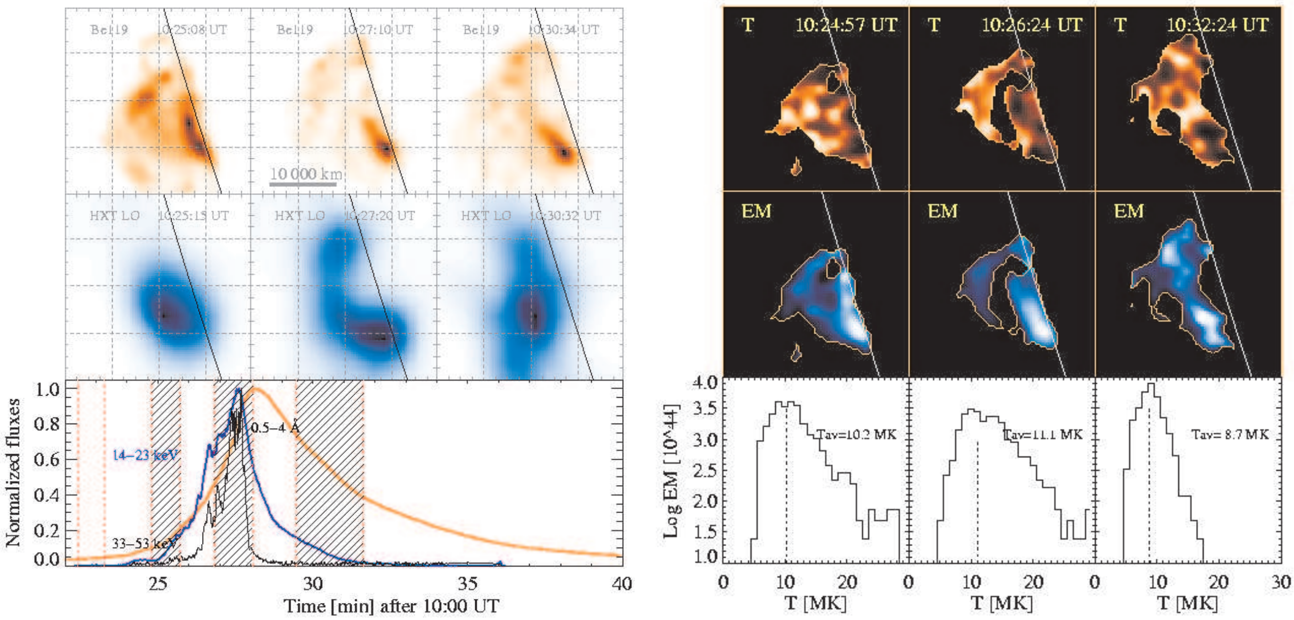

Fig. 5. *Left: The composite of Be119 SXT deconvolved images (top row) and corresponding in time MEM reconstructed LO HXT images (middle row) for three moments during the 18 December 1991 flare evolution. The soft (GOES) and hard (LO and M1 HXT) X-ray normalised lightcurves are displayed in the bottom row. The hatched areas denote time intervals when the HXT fluxes have been integrated in order to reconstruct the images displayed in the middle row. Right: The distribution of main thermodynamic parameters (temperature - top row, emission measure - middle row and "quasi-differential" emission measure histogram - bottom row) for three moments (respective columns) during the flare evolution. The size of each frame is* (40×40) *arcsec.*

that the time profile of hard X-ray emission represented by HXT L channel flux resembles the soft X-ray emission (SXT Al12 and Be119 fluxes) for the North footpoint (left column) the best. The double maximum can be recognised in both hard and soft X-ray lightcurves at the same time. The observed differences of physical conditions at footpoint and summit (coronal) areas can be useful in order to distinguish between them for disc flares which may not be obvious because of projection effects. Identification of kernels for disc flares can lead to better reconstruction of the magnetic field lines "connectivity" pattern in the corona.

Using the deconvolved images and incorporating fine image alignment technique we were able to determine the maps of distribution of important physical parameters in flares. An example is shown in Figure 5 (right panel). In the left panel the deconvolved soft (SXT Be119) and MEM reconstructed hard (HXT LO channel) X-ray images for three selected times during the evolution of the flare on 18 December 1991 are shown. At the bottom the lightcurves (GOES and HXT LO and M1 channels) are presented. The two upper rows on the right panel present (in the false colours) the maps of plasma temperature and emission measure for three times. The areas embraced by the solid curve are those, common in Al12 and Be119 images for which the count rate is above 30 DN/subpixel (i.e. 750 DN/pixel). In the lowest row the "quasi" differential emission measure distributions (QDEM) together with the average temperature of the region are presented. The QDEM histogram has been constructed based on the temperature and emission measure maps. First the elements (subpixels) have been identified where the temperature falls into $(T, T+1)$ MK range. Next the emission measures for those elements have been summed and plotted on the vertical axis of the histogram for appropriate temperature ranges. It is seen that the bulk of plasma in the flaring region is characterised by the relatively high temperature around 10 MK. (One must remember that using Al12 and Be119 filters ratio technique the plasma with temperatures higher than 5 MK can only be probed.) The average temperatures for the entire areas selected are indicated in the Figure. As may be expected the average temperature is the lowest (8.7 MK) during flare decay phase. The corresponding average densities are: 7.6 x 10^{10}, 1.1 x 10^{11} and 1.4 x 10^{11} cm^{-3} respectively. Presence of small amount of plasma with temperatures above 20 MK during the rise phase (the left and middle histogram) is common. This high temperature tail in QDEM distribution is not seen during the decay phase. The high temperature component fades away after the main hard X-ray phase. It may be responsible for the radiation observed in the Fe XXV emission line on the

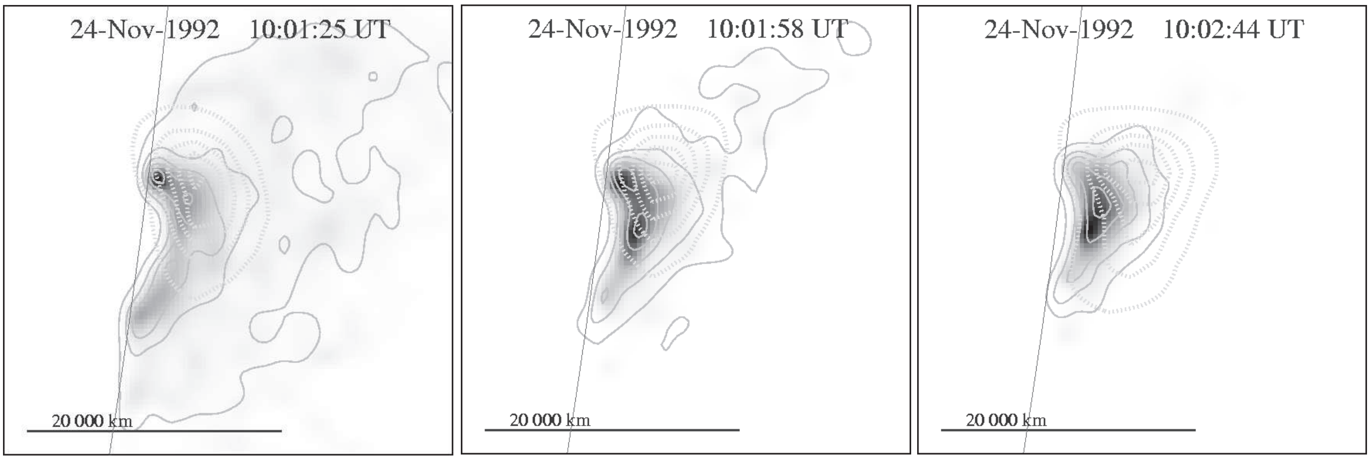

Fig. 6. *The comparison of the soft and hard brightest area locations for three moments during the rise phase of the flare on 24 November 1992 at* $\sim$ 10 *UT. At the base the Al12 deconvolved images are presented for the times indicated. The solid line contours correspond to Be119 SXT images while the dashed contours for the M1 channel of HXT images.*

spectra recorded by BCS.

The other important problem which can be investigated based on deconvolved SXT images is the detailed examination of spatial relationship between the soft and hard X-ray emission patches. As is presently known they do not exactly overlap. The hard X-ray sources are usually placed above the corresponding maxima of softer emission both for the summit and footpoint regions. This can be seen in the two upper rows of the left panel in Figure 5. In Figure 6 the relative location of soft X-ray emission (seen on deconvolved SXT images) and hard X-ray one (seen on the MEM reconstructed HXT images) are presented which confirm these earlier findings unambiguously. In the Figure the three frames obtained during the rise phase of the flare on 24 November 1992 at $\sim 10:02$ UT are shown. It is seen that the soft and hard X-ray emission patches are not co-spatial and the distance of their centres increases with time during $\sim$ 70 sec of evolution presented.

As a last point we would like to stress that presence of persistent bright regions seen in the most flares observed by *Yohkoh* are hard to accommodate within proposed simple flare scenarios which has been pointed out by many authors. The team from the Astronomical Institute of Wroclaw University (headed by prof. J. Jakimiec) has worked out a flare model based on the hypothesis that the turbulent energy release in solar flares takes place inside entire volume of each kernel. This concept can help in resolving the problem of incompatibility of existing flare observations and theoretical scenarios. In a series of contributions (Jakimiec, 1998, 1999, 2001a, b) it has been argued that flare kernels are strongly turbulent regions with tangled magnetic lines undergoing volumetric reconnections in many places at the same time. Khan et al. (1995) has added important supporting evidence to this hypothesis. They found significant non-thermal (turbulent) motions for loop-top flare kernels when investigating limb flares with only top kernel visible from behind the limb. In Jakimiec model the turbulent flare kernels are supposed to be filled up with a number of tiny turbulent reconnection/acceleration regions and thus the energy is expected to be released simultaneously in many closely packed transient current sheets within kernel's volume. Inside the kernels the energy is transported by the turbulent plasma motions. It has been shown that it is easy to produce turbulent kernel in typical active region magnetic topology. Mixed magnetic polarities and their dynamics in young active regions cause that the probability of interaction of three or even more flux tubes is high there. If this happens the cascade of reconnections may develop with many transient reconnection regions where the magnetic energy is dissipated efficiently. According to this hypothesis the MHD turbulence is the basic mechanism of flare energy release. It also gives a chance to explain the huge flux of the accelerated electrons which is responsible for generation of the observed hard X-ray flare radiation. It is postulated by Jakimiec that the regions responsible for the most efficient particle acceleration are kernel boundaries, where the high-speed turbulence interacts with the surrounding magnetic fields. The plasma turbulence at the loop-top has been regarded as important acceleration mechanism of electrons produced during the solar flares also in the paper by Fletcher (1999).

CONCLUDING REMARKS

Results of inspection of imaging data from recent missions like *Yohkoh*, *SOHO* and *TRACE* emphasize the well-known fact that the solar corona is highly structured. Additionally interpretation of the *Yohkoh* data resulted in a consensus that the kernels are the dominant emitting structures of flare events. One may conclude that there are NO simple flares. The simplicity of *GOES* soft X-ray lightcurves for flares is misleading. Complexity of the soft X-ray sources is evident from SXT, *SOHO* and *TRACE* observations. High resolution ground observations and hard X-ray flux variability provide additional arguments in favour of elementary flare complexity. Persistent presence of loop-top kernels is hard to understand within widely accepted chromospheric evaporation flare scenario. The studies of morphology and thermodynamic of flaring regions based on deconvolved SXT images led us to the conclusion that the non uniformities are present in both density and temperature within these kernels. They must be a direct result of spatial and temporal variations in the rate of volumetric flare heating. Despite the fact that the *major* progress has been made recently in the field of solar flares we are still far from complete understanding of the detailed mechanism of energy build up and release. It is evident that current observations of flares still lack the spatial resolution to support present theoretical models. It is said again and again that fast imaging with better than 0.1 arcsec resolution over a small field of view, together with a wide energy coverage and with support of spectrographic observations seem to be needed in order to investigate the distribution of temperature and density together with magnetic and velocity fields. This will allow energy release, transport and dissipation process to be studied in more detail. A major effort of the international solar physics community for the next decade will be the Solar-B space mission. However the presence of a turbulent regime within the flaring kernels can not be observationally confirmed even by Solar-B since the range of scales associated with the dissipation of energy and cascade are expected to operate on spatial scales still beyond present-day spatial resolution limit. Only missions currently in the planning stage aimed for an angular resolution of the order of a TENTH of arcsec would possibly permit for such observations.

ACKNOWLEDGEMENTS

This work has been supported by the Grant 2.P03D.024.17 of Polish Committee for Scientific Research.

REFERENCES

Acton, L.W., Feldman, U., Bruner, M.E., Doschek, G.A., Hirayama, T. *et al.*, The Morphology of 20×10^6 K Plasma in Large Non-Impulsive Solar Flares, *Publ. Astron. Soc. Japan,* **44**, L71, (1992).

Doschek, G.A., The Electron Temperature and Fine Structure of Soft X-ray Solar Flares, *Astrophys. J.,* **527**, 426, (1999).

Doschek, G.A., Strong, K.T., & Tsuneta, S., The Bright Knots at the Tops of Soft X-ray Flare Loops: Quantitative Results, *Astrophys. J.,* **440**, 370, (1995).

Feldman, U., Hiei, E., Phillips, K.J.H., Brown, C.M., & Lang, J., Very Impulsive Solar Flares Observed with the Yohkoh Spacecraft, *Astrophys. J.,* **421**, 843, (1994a).

Feldman, U., Seely, J.F., Doschek, G.A., Strong, K.T., Acton, L.W. *et al.*, The Morphology of the 10 MK Plasma in Solar Flares: Nonimpulsive Flares, *Astrophys. J.,* **424**, 444, (1994b).

Fletcher, L., Looptop Hard X-ray Sources, *ESA SP-448*, 693, (1999).

Fludra, A., Jakimiec, J., Tomczak, M., Culhane, L.J., & Acton, L.W., Long Duration Events in Magnetic Arcades and Large Loops, *NRO, Report No. 360,* 393, (1994).

Foukal, P.V., The Pressure and Energy Balance of the Cool Corona over Sunspots, *Astrophys. J.,* **210**, 575, (1976).

Golub, L., Structure of the Solar X-ray Corona, *ASP Conference Series,* **26**, 193, (1992).

Golub, L., Difficulties in Observing Coronal Structures, *Solar Phys.,* **174**, 99, (1997).

Golub, L., Herant, M., Kalata, K., Lovas, I., Nystrom, G. *et al.*, Sub-arcsecond Observations of the Solar X-ray Corona, *Nature,* **344**, 842, (1990).

Gomez, D.O., Martens, P.C.H., & Golub, L., Normal Incidence X-ray Telescope Power Spectra of X-ray Emission from Solar Active Regions. II. Theory, *Astrophys. J.,* **405**, 773, (1993).

Harra-Murnion, L.K., Culhane, J.L., Hudson, H.S., Fujiwara, T., Kato, T., & Sterling, A.C., Isolating the Footpoint Characteristics of a Solar Flare Loop, *Solar Phys.,* **171**, 103, (1997).

Herant, M., Pardo, F., Spiller, E., & Golub, L., Flares Observed by the Normal Incidence X-ray Telescope on 1989 September 11, *Astrophys. J.,* **376**, 797, (1991).

Hudson, H.S., Strong, K.T., Dennis, B.R., Zarro, D., Inda, M. *et al.*, Impulsive Behavior in Solar X-radiation, *Astrophys. J.,* **422**, L25, (1994).

Jakimiec, J., What we Can learn from X-ray Observations of Stellar Flares, *Physica Scripta,* **T77**, 137, (1998).

Jakimiec, J., Tomczak, M., Falewicz, R., Phillips, K.J.H., & Fludra, A., The Bright Loop-Top Kernels in Yohkoh X-ray Flares, *Astron. Astrophys.,* **334**, 1112, (1998).

Jakimiec, J., Turbulent Energy Release in Solar Flares, *ESA SP-448,* 729, (1999).

Jakimiec, J., Small-Scale Reconnection in Solar Flares, *Adv. Space Res.,* accepted, (2001a).

Jakimiec, J., Energy Release in Solar Flares, *Adv. Space Res.,* accepted, (2001b).

Khan, J.I., Harra-Murnion, L.K., Hudson, H.S., Lemen, J.R., & Sterling, A., Yohkoh Soft X-ray Spectroscopic Observations of the Bright Loop-Top Kernels, *Astrophys. J.,* **452**, L153, (1995).

Masuda, S., Kosugi, T., Hara, H., Tsuneta, S., & Ogawara,Y., A Loop-Top Hard X-Ray Source in a Compact Solar Flare as Evidence for Magnetic Reconnection, *Nature,* **371**, 495, (1994).

McTiernan, J.M., Kane, S.R., Loran, J.M., Lemen, J.R., Acton, L.W., *et al.*, Temperature and Density Structure of 1991 November 2 Flare Observed by the Yohkoh Soft X-ray Telescope and Hard X-ray Telescope, *Astrophys. J.,* **416**, L91, (1993).

Nitta, N.V., Sato, J., & Hudson, H.S., The Physical Nature of the Loop-Top X-ray Sources in the Gradual Phase of Solar Flares, *Astrophys. J.,* **552**, 821, (2001).

Roumeliotis, G., A Novel Maximum-Likelihood Method of Image Reconstruction with Increased Sampling, *Astrophys. J.,* **452**, 944, (1995).

Sams III, B.J., Golub, L., & Weiss, N.O., X-ray Observations of Sunspot Penumbral Structure, *Astrophys. J.,* **399**, 313, (1992).

Sheeley, Jr. N.R., Bohlin, J.D., Brueckner, G.E., Purcell, J.D., Scherrer, V., & Tousey, R., XUV Observations of Coronal Magnetic Fields, *Solar Phys.,* **40**, 103, (1975).

Siarkowski, M., Sylwester, J., Jakimiec, J., & Tomczak, M., Improvement of SXT Image Alignment in Order to Obtain High-Resolution Temperature Maps, *Acta Astron.,* **46**, 15, (1996).

Sylwester, J., High-Resolution Temperature Maps of Flares from Deconvolved SXT Images, *JOSO Annual Report '95,* 131, (1995).

Sylwester, J., Sylwester, B., & Siarkowski, M., ANDRIL Algorithm for Deconvolution of SXT Images, *ASP Conference Series,* **111**, ed. by R.D. Bentley & J.T. Mariska, 244, (1996a).

Sylwester, B., Sylwester, J., & Siarkowski, M., Fine Structures Observed on Deconvolved SXT Images, *ASP Conference Series,* **111**, ed. by R.D. Bentley & J.T. Mariska, 249, (1996b).

Sylwester, J., & Sylwester, B., ANDRIL - Maximum Likelihood Algorithm for Deconvolution of SXT Images, *Acta Astron.,* **48**, 519, (1998a).

Sylwester, J., & Sylwester, B., Evolution of Flaring Structures, *ASP Conference Series,* **155**, ed. by C.E. Alissandrakis & B. Schmieder, 381, (1998b).

Sylwester, B., & Sylwester, J., Physical Conditions in Flaring Loops, *JOSO Annual Report '97,* 97, (1998c).

Sylwester, J., & Sylwester, B., Reconstruction of Images with Poisson Noise, *Acta Astron.,* **49**, 189, (1999a).

Sylwester, B., & Sylwester, J., Reconstruction of Coronal Magnetic Fields from Deconvolved SXT Images, *JOSO Annual Report '98,* 105, (1999b).

Sylwester, B., & Sylwester, J., Flaring Structures Observed in Deconvolved SXT Images, *Acta Astron.,* **49**, 85, (1999c).

Sylwester, B., & Sylwester, J., The Properties of Flares Produced within AR 6919, *ESA SP-448,* 895, (1999d).

Sylwester, B., & Sylwester, J., Physical Conditions within Flare Kernels, *Adv. in Space Res.,* accepted, (2001a).

Sylwester, B., & Sylwester, J., Thermodynamics of Partly Occulted Limb Flares, *ESA SP-477,* accepted, (2001b).

Sylwester, J., and Sylwester, B., Behind the Limb X-ray Sources as Seen by Yohkoh, *this issue*, (2002).

Tomczak, M., The Impulsive Phase of the Arcade Flare of 28 June 1992, 14:24 UT, *Astron. Astrophys.,* **317**, 223, (1997).